PCCP

Accepted Manuscript

ROYAL SOCIETY OF CHEMISTRY

www.rsc.org/pccp

Journal Name

RSCPublishing

ARTICLE

Cite this: DOI: 10.1039/x0xx00000x

Homodimeric BODIPY Rotor as a Fluorescent Viscosity Sensor for Membrane-Mimicking and Cellular Environments

Received 00th January 2012,
Accepted 00th January 2012

DOI: 10.1039/x0xx00000x

www.rsc.org/

Sangram Raut[1], Joseph Kimball[1], Rafal Fudala[2], Hung Doan[1], Badri Maliwal[2], Nirupama Sabnis[3], Andras Lacko[3], Ignacy Gryczynski[2], Sergei V. Dzyuba[4], Zygmunt Gryczynski*[,1,2]

Fluorescence properties of a novel homodimeric BODIPY dye rotor for Fluorescence Lifetime Imaging Microscopy (FLIM) are reported. Steady state and time resolved fluorescence measurements established the viscosity dependant behaviour *in vitro*. Homodimeric BODIPY embedded in different membrane mimicking lipid vesicles (DPPC, POPC and POPC plus cholesterol) demonstrated to be a viable sensor for fluorescence lifetime based viscosity measurements. Moreover, SKOV3 cells readily endocytosed the dye, which accumulated in membranous structures inside cytoplasm thereby allowing viscosity mapping of internal cell components.

Introduction

A variety of mass and signal transport phenomena as well as intermolecular interactions are often governed by viscosity[1, 2]. As such, it is important to be able to measure/estimate viscosity and detect the changes in viscosity upon exposure to a stimulus. In view of synthetic accessibility, molecular viscometers are attractive probes for sensing the viscosity of various environments[3-5].

Fluorophore dyads/dimers, which are small molecular probes with two fluorescent moieties, is an interesting class of molecular viscometer, which have found numerous applications in ratiometric sensing of analytes, cascade-type energy transfer events and chemical transformations[6-9]. The spectroscopic properties of these types of systems, including extinction coefficients, apparent brightness and Stokes shifts, could be tuned *via* structural and functional modification of the monomeric fluorophores, and further accentuated by the dyad's structure. Since many biochemical applications are hindered by the lack of suitable structurally diverse fluorophores, the access to dyads, which rely on facile and modular synthetic approaches allowing for the formation of both homodimeric and heterodimeric systems, might provide a viable solution.

BODIPY dyes are versatile fluorophores whose spectral properties can be tuned *via* a range of structural modifications[10, 11]. As a result, BODIPY dyes have been explored in a variety of applications, including molecular, ionic and biological sensing[12-15]. Importantly, BODIPY-based rotors have been shown to be suitable for sensing viscosity, including the viscosity of intracellular environments. Specifically, BODIPY dyes with the modification on the *para*-position of the phenyl substituent in the *meso*-position of the BODIPY scaffold were shown to be viable sensors of intracellular viscosity as their fluorescent lifetime showed a good correlation with viscosity[16-19]. It should be noted that so-called "distorted-BODIPY" fluorescent viscometer with the carboxyaldehyde-moiety in the *meso*-position of the BODIPY-scaffold was shown not only to map the viscosity of the cell, but also to detect viscosity changes associated with the early stages of apoptosis in a breast cancer cell line MCF-7[20]. In regard to the BODIPY-based dyads for measuring intracellular viscosity, the coumarin-BODIPY dyad was demonstrated to detect viscosity in mitochondria[21]. In view of the significant linear correlation of both fluorescence intensity and fluorescence lifetimes with viscosity, the aforementioned sensor was shown to be applicable for monitoring viscosity changes that occurred during mitochondrial apoptosis events. Overall, it could be argued that fairly long fluorescence lifetimes (on the order of several ns) along with synthetic accessibility make BODIPY-containing systems a viable platform for development of fluorescence lifetime based molecular viscometers.

It should be pointed out that multistep synthetic protocols that are employed for the preparation of the dyads (BODIPY-based[21] as well as porphyrin-based, which have proven to be very potent in mapping cellular viscosity[22]) should be taken into consideration and they often might be viewed as a drawback. In order to overcome this drawback, we decided to

explore homodimeric BODIPY dyes, which could be prepared in a few steps from readily available starting materials. Towards this end, we recently assessed the potential of a BODIPY dimer to act as viscometer for molecular and ionic solvents (Figure 1)[23]. Here, we expand on the application of the BODIPY dimer and report on its ability to act as a microviscosity sensor in various cellular and membrane-mimicking environments.

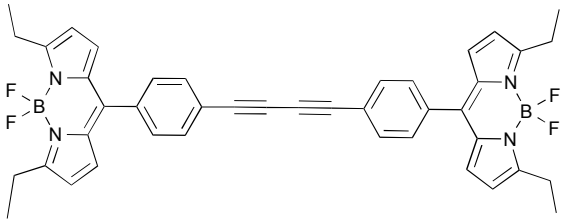

Figure 1: Chemical structure of BODIPY homodimer

Materials and Methods

BODIPY Dyad Synthesis

All chemicals and solvents were obtained from commercial sources; they were of highest grade possible and were used as received. BODIPY homodimer was prepared according to literature procedure[23], and exhibited spectral properties consistent with the structure: ^{1}H NMR (400 MHz, $CDCl_3$): δ = 7.68 (d, *J* = 8.4 Hz, 2H), 7.53 (d, *J* = 8.4 Hz, 2H), 6.75 (d, *J* = 4.2 Hz, 2H), 6.40 (d, *J* = 4.3 Hz, 2H), 3.11 (q, *J* = 7.6 Hz, 4H), 1.38 (t, *J* = 7.6 Hz, 6H); ^{19}F NMR (376 MHz, $CDCl_3$): δ = 145.24 (q, *J* = 32.7 Hz).

Spectroscopic Measurements

UV-Vis absorption and fluorescence spectra were obtained using a Cary 50 bio UV–visible Spectrophotometer (Varian Inc.) and Cary Eclipse Spectrofluorometer (Varian Inc.) respectively. All the measurements were done in 0.4mm X 1cm quartz cuvettes at room temperature with optical density below 0.05, unless mentioned otherwise. In order to measure the quantum yield, absorption spectra of BODIPY dimer was collected followed by measuring the integrated fluorescence intensity of the sample. A solution of fluorescein in 0.1 M NaOH was used as a reference (quantum yield: 0.90)[24]. Fluorescence lifetime was measured on a FluoTime 200 fluorometer (PicoQuant, Inc.) using a 470nm diode laser. The fluorometer was equipped with an ultrafast microchannel plate detector (MCP) from Hamamatsu, Inc. The fluorescence lifetimes were measured in the magic angle condition and data analyzed using FluoFit4 program from PicoQuant, Inc (Germany) using multi-exponential fitting model:

$$I(t) = \sum_i \alpha_i e^{-t/\tau_i} \qquad (1)$$

where, α_i is the amplitude of the decay of the i^{th} component at time t and τ_i is the lifetime of the i^{th} component. The intensity weighted average lifetime (τ_{Avg}) was calculated using the following equation:

$$\tau_{avg} = \sum_i f_i \tau_i \quad \text{where} \quad f_i = \frac{\alpha_i \tau_i}{\sum_i \alpha_i \tau_i} \qquad (2)$$

Radiative (K_r) and non-radiative (K_{nr}) rates were calculated using experimentally measured quantum yield and fluorescence lifetimes using the following equation:

$$\phi_f = \frac{K_r}{K_r + K_{nr}} \quad \text{and} \quad \tau = \frac{1}{K_r + K_{nr}} \qquad (3)$$

Preparation of Lipid Vesicles

Three different lipid unilamellar vesicles were prepared using DPPC (1, 2-dihexadecanoyl-*sn*-glycero-3-phosphocholine), POPC (1-hexadecanoyl-2-(9Z-octadecenoyl)-*sn*-glycero-3-phosphocholine) and POPC +Cholesterol. Appropriate amounts of each lipid and BODIPY homodimer were dissolved in chloroform (lipid:dye ratio was 800:1) in glass bottles. The solvent was evaporated under oxygen free nitrogen stream and left overnight to remove any traces of organic solvents. Next, PBS (phosphate buffer saline) was added followed by strong sonication at about 40 ^oC to get giant multilamellar vesicles. Moreover, in order to obtain unilamellar vesicles, mutlilamellar vesicles were passed through 100 μm and 0.02 μm membrane syringe filters. As obtained lipid vesicles were used for fluorescence lifetime measurements.

Fluorescence Microscopy and FLIM

SKOV3 overian carcinoma cell line obtained from American Type Culture Collection (ATCC), Manassas, VA (USA) was grown to 70 % confluence in RPMI supplemented with 10 % FBS and 1 % Pen-Strep. Cells were trypsinized using 0.25 % Trypsin EDTA and seeded on 20 mm round glass-bottom petri dishes. After 24 hours, cells were stained with 500nM of BODIPY for 20 min at 37 °C followed by FLIM imaging on Olympus IX7 microscope. Laser excitation was provided by a pulsed laser diode (PDL-470) emitting 470 nm light and driven by a PDL 828 "Sepia II" driver. This driver was operated at 80 MHz. Measurements were performed on a MicroTime 200 time-resolved, confocal microscope by PicoQuant. The excitation and emission light was focused by a 60X 1.2 NA Olympus objective in an Olympus IX71 microscope, and the emission light was filtered by a 488 long wave pass filter before passing through a 50 μm pinhole. Detection was made by a hybrid photomultiplier assembly. The resolution of the time correlated single photon counting (TCSPC) module was set to 4 ps/bin in order to facilitate the detection at the highest possible resolution. All data analyses were performed using the SymPhoTime software, version 5.3.2. All experimental equipment and the SymPhoTime software were provided by PicoQuant, GmbH as part of the MicroTime 200 system.

Theory

In typical molecular rotors, a non-radiative pathway responds strongly to viscosity in the immediate vicinity of the rotor. Twisting or rotation within the molecular structure is the prime reason behind viscosity dependent behavior. A decrease in the non-radiative rate with increasing viscosity results in a sharp

increase in fluorescence quantum yield and fluorescence lifetime. In those cases where the spectroscopic characteristics of the probe are viscosity dependent, a linear dependence of the quantum yield as a function of viscosity should be observed. This viscosity dependence of quantum yield can be expressed using Forster-Hoffman theory[26]:

$$\ln(\phi_f) = C + x\ln(n) \qquad (4)$$

where n is the viscosity and x is the slope, which is 0.6 for a perfect rotor as predicted by the Forster-Hoffman theory. However, the main problem associated with using quantum yield – viscosity correlations is the inability to differentiate between viscosity and other factors, such as local dye concentration, that might affect the steady state intensity, and thus the quantum yield. On the other hand, fluorescence lifetime can be utilized for the viscosity dependence without the aforementioned concern. Notably, a Forster-Hoffman equation is also applicable to lifetime and viscosity as:

$$\ln(\tau) = C' + y\ln(n) \qquad (5)$$

This equation serves as a basis to visualize the intracellular viscosity. A calibration curve of viscosity *versus* lifetime can be constructed using media of different viscosities and subsequently applied to map the viscosity inside the cells.

Results and Discussion

Photo-physical Characterization

Our goal was to establish whether a simple BODIPY homodimer could act as a molecular rotor, with its fluorescence emission and fluorescence lifetime being sensitive to the ambient viscosity. It appeared that changing the viscosity of the media (by using ethanol–glycerol mixtures[25]) did not significantly affect the shape and peak emission wavelength (Figure 2A). A small shift of the emission maximum (~7 nm) was observed when viscosity changed from that of ethanol to that of glycerol and this could be ascribed to slight changes of the media polarity. Additionally,

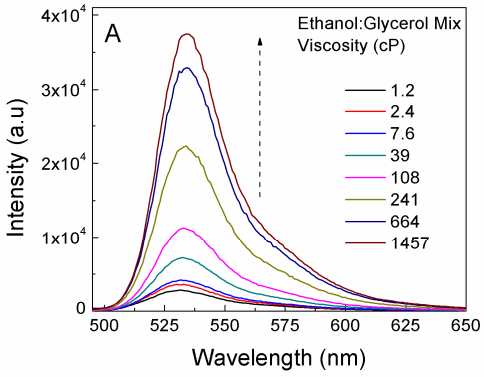

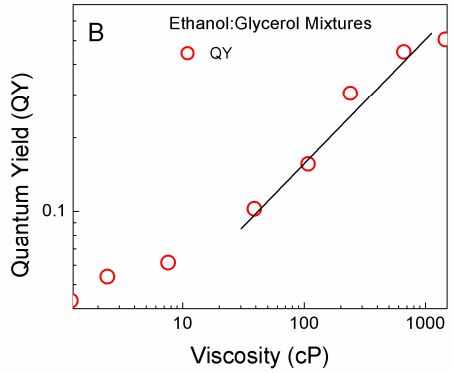

Figure 2: A) Emission spectra of BODIPY dimer in different viscosity mixtures of ethanol:glycerol. B) Log-log plot of quantum yield and viscosity.

increasing the viscosity of the media increased the emission intensity and fluorescence quantum yield, which is consistent with Equation 4. The value of Φ_f, as a function of viscosity in ethanol:glycerol mixtures is shown in Figure 2B. Linear dependence of viscosity in regard to the Φ_f of the BODIPY dimer was observed for viscosities above 20 cP.

Fluorescence intensity decays at increasing viscosity in ethanol : glycerol mixtures were measured (Figure 3A) and the fluorescence lifetime changed distinctly as a function of viscosity (Figure 3B).

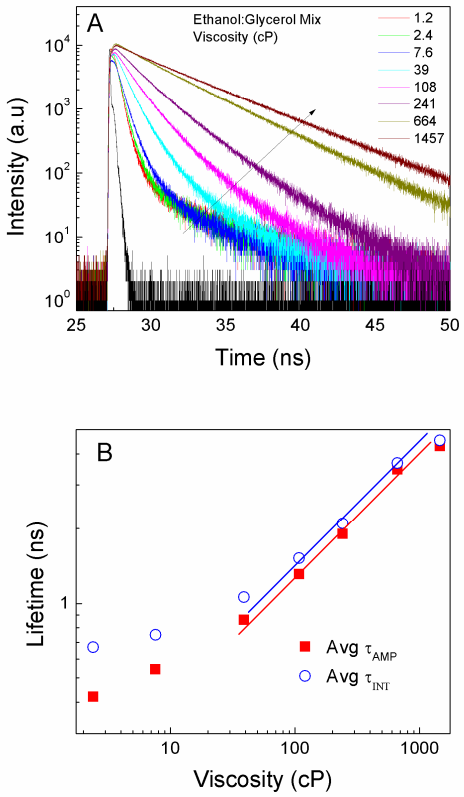

Figure 3: A) Fluorescence intensity decays of BODIPY dimer in different viscosity mixtures of ethanol:glycerol. B) Average fluorescence lifetime as a function of viscosity.

Similar to quantum yield, linear dependence was observed for media's viscosity above 20 cP. Specifically, fluorescence lifetime in ethanol (1.2 cP) was 340 ps, while in glycerol (1457 cP) the fluorescence lifetime increased to 4.3 ns. The fluorescence lifetimes at viscosities between 1.2 to 1457 cP were all above 300 ps. This is important, since the lower limit for lifetime resolution of our TCSPC (most of time-resolved systems available today) is significantly below 300 ps. Considering Equation 5, it was expected that the plot should have produced a linear dependence between lifetime and log-viscosity. Indeed, this was confirmed at viscosities above 20 cP giving slope of 0.46. This value compared well with the value of 2/3 predicted by Forster and Hoffmann[26]. Typical slope values range from 0.2 to 1.4 for different rotors[27]. We found that below 20 cP, the fluorescence lifetime and quantum yield were minimally variant. Arguably, the viscosity dependent rotational resistance for BODIPY units in the dimer became insignificant at lower viscosities.

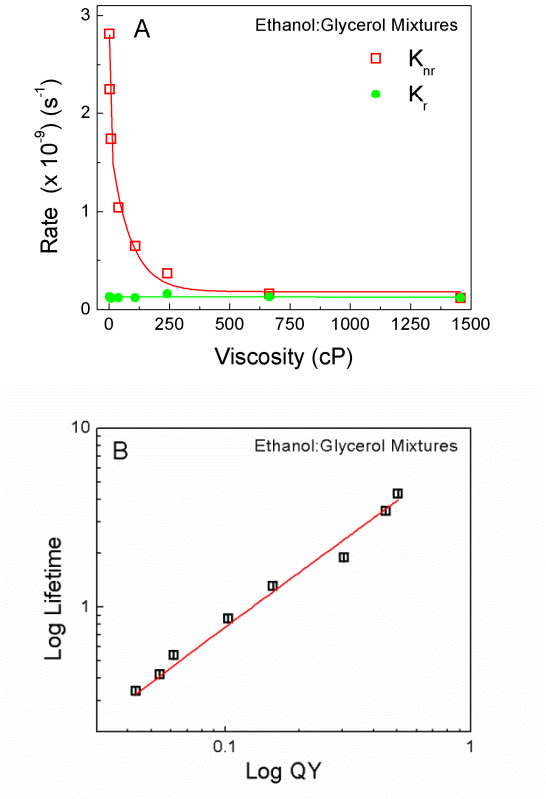

Figure 4: A) Radiative and non-radiative rates of BODIPY dimer in ethanol:glycerol mixtures as a function of viscosity. B) Log-log plot of average fluorescence lifetime and quantum of yield of BODIPY dimer obtained from different ethanol:glycerol mixtures.

The rate constants K_r and K_{nr} were calculated from the experimentally measured quantum yields and fluorescence lifetime, using Equation 3. In ethanol, quantum yield was 0.02 and it increased significantly as the viscosity of the solution increased, as expected based on the Equation 4. Moreover, the value of K_r remained steady as a function of the viscosity; however, the value of K_{nr} decreased sharply with increasing viscosity up to 375 cP (Figure 4A). This suggested that the increase in quantum yield with increasing viscosity was due to the suppression of non-radiative processes. Although the exact orientation of phenyl rings in relation to the plane of the BODIPY core remains to be clarified, it is arguable that the viscous environment prevented access to non-emissive state by restricting the rotation of the BODIPY units around the diyne moiety. Efforts are underway to determine the absorption and emission transition moments of the BODIPY dimer, which will further enlighten the exact mechanism of this molecular rotor. The complete viscosity dependence was further confirmed by the linear dependence of log quantum yield *versus* log lifetime (Figure 4B).

A

Lipid Vesicles	τ_{AMP} / ns	τ_{INT} / ns	Viscosity /cP
DPPC	1.30	1.93	200
POPC	1.54	2.07	220
POPC+cholesterol	1.62	2.20	260

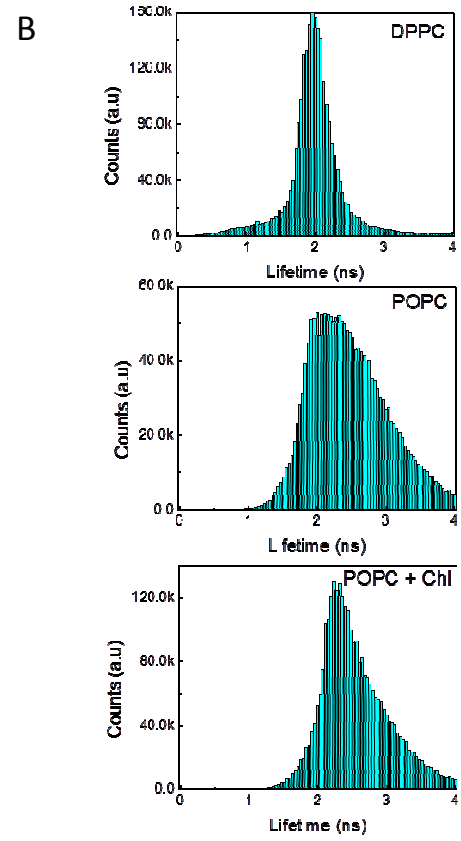

Figure 5: A) Table shows the average fluorescence lifetimes of BODIPY dimer obtained in different lipid vesicles and calculated corresponding viscosities. B) Lifetime distribution of BODIPY dimer from lipid vesicles.

Prior to the cellular studies, we envisioned that investigations using simple lipid vesicles would be advantageous for further understanding of the cellular observations. Thus, encapsulation of BODIPY dimer into vesicles, which were made from different lipid components and physical states, could give an

idea about the possible position of the dye molecules in lipid bilayers and their surrounding micro-viscosity from fluorescence lifetime measurements. Thus, the lifetime data of BODIPY dimer in DPPC, POPC and POPC+cholesterol was evaluated (Figure 5A). It appeared that average lifetimes did not vary significantly, except that POPC+cholesterol was found to be longer owing to a comparatively rigid membrane structure (Figure 5B). Moreover, examining the lifetime distributions, DPPC indicated the presence of a more ordered lipid structure (as evident from narrow lifetime distribution) whereby molecules were oriented in certain (well-ordered) way compared to other two lipid vesicles. POPC showed a wider lifetime distribution attributed to different micro-viscosities experienced by BODIPY dimer in vesicles due to less ordered lipid molecules in those vesicles.

We envisioned that using the fluorescence lifetime *versus* viscosity calibration plots obtained in ethanol:glycerol mixtures (Figures 2 – 4) would allow us to determine the viscosity distribution in cells *via* FLIM. Even though the fluorescence lifetime of a fluorophore could be influenced by several environmental parameters apart from viscosity, such as refractive index, polarity, pH, or chemical and physical quenching processes**,** it was shown that BODIPY dyes were insensitive to changes of such environmental parameters and can be unambiguously used to probe the intracellular viscosity[18, 28].

Fluorescence Microscopy and FLIM

BODIPY dimer was readily taken up by the SKOV3 cells. A bright punctate distribution of the dye was observed throughout the cells. Moreover, very low intensity regions in cytosols were also present. We expected BODIPY dimer to target the hydrophobic membrane regions owing to its hydrophobic nature as seen from lipid vesicle experiments. Punctate distribution appeared to be due to the accumulation of the dye in certain cell organelle membranes (Figure 6A). This distribution pattern was found to be similar to the one observed

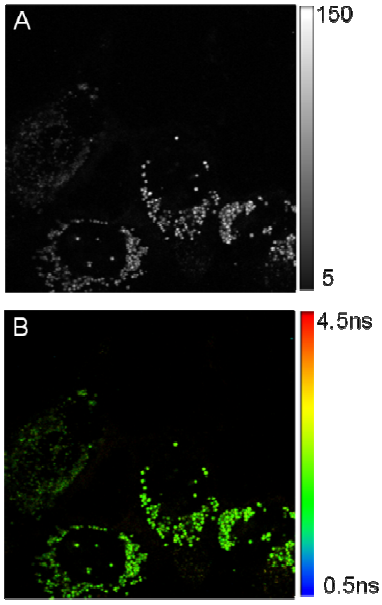

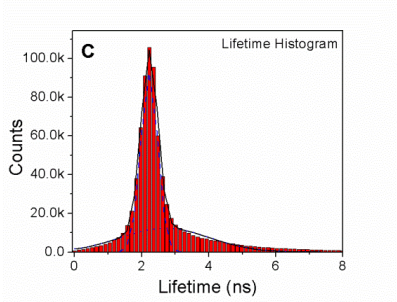

Figure 6: A) Confocal intensity image (80X80 µm) SKOV3 cells treated with BODIPY dimer. B) FLIM image of SKOV3 cells treated with BODIPY dimer. C) Lifetime distribution of SKOV3 cells treated with BODIPY dimer obtained in figure 6B.

by Levitt *et al.,*[18] difference being less intense cytosolic fluorescence in our case. The lifetime distribution of the dye was examined after 20 min of the incubation time Furthermore, with longer dye incubation time (1 h), no significant differences in distribution of the BODIPY dimer inside cells were observed. It is possible tht the dye uptake mechanism might be a passive diffusion since the endocytotic uptake is energy dependent, yet the exact dye uptake mechanism remains to be clarified.

Following the calibration of fluorescence lifetimes of BODIPY dimer as a function of viscosity, we performed FLIM analysis to generate spatial map of viscosity in SKOV- 3 cells incubated with BODIPY dimer (Figure 6B). Similar to the higher viscosity mixtures (ethanol:glycerol), the fluorescence decay in each pixel could be fitted with bi-exponential distribution model. Earlier, we used such a model to study different conformational properties of adrenergic receptors[29]. We obtained a histogram of fluorescence lifetimes across the whole image by graphing the lifetime distribution extracted from the image (Figure 6C). The histogram showed the bi-modal distribution of the dye. By using Gaussian fit, individual contributions to the histogram were 2.2 ns and 2.6 ns. Such lifetime distributions might indicate two distinctly different dye populations associated with different properties of the environments. Major part (*ca*. 90 %) was contributed by 2.2 ns with narrow FWHM, which was associated with the bright punctate distribution and appears to be located in the vesicular structures. The wider distribution of lifetime (2.6 ns peak) is due to the random distribution of BODIPY dimer inside cytoplasm and other cellular organelles (distribution of viscosities). The measured fluorescence lifetime inside cells lied within the linear range of the viscosity calibration plot. According to the calibration curve, the 2.2 ns lifetime appeared to correspond to the viscosity of *ca.* 260 cP

The initial observation of the dye distribution indicated that these organelles could be either mitochondria or lysosomes. Thus, we decided to carry out the co-localization experiment using respective fluorescent markers and BODIPY homodimer (Figure 7): the two individual channels for BODIPY dimer and Mitotracker along with co-localization analysis showed partial overlap among them. Similar results were obtained using Lysotracker and BODIPY dimer (Figure 8). These observations suggested that BODIPY rotor also accumulated in organelles other than mitochondria and lysosomes and thus exhibited nonspecific cell targeting.

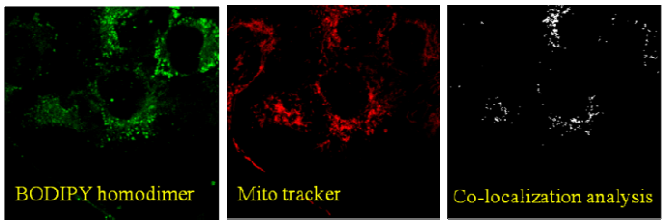

Figure 7: Left panel: SKOV-3 cells treated with BODIPY dimer, Middle panel: SKOV-3 cells treated with Mitootracker and Right panel: Co-localization analysis of both dyes using ImageJ.

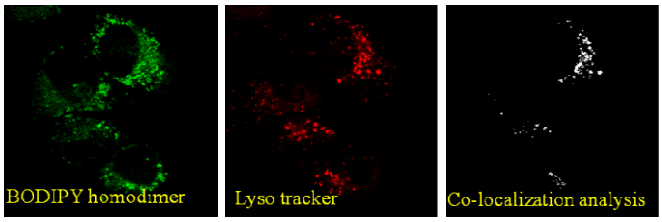

Figure 8: Left panel: SKOV-3 cells treated with BODIPY dimer, Middle panel: SKOV-3 cells treated with Lysotracker and Right panel: Co-localization analysis of both dyes using ImageJ.

Conclusions

In conclusion, we have reported on a novel, easily accessible homodimeric BODIPY as a steady state and time resolved viscosity sensitive molecular rotor, which allowed mapping the viscosity by nonspecifically staining the intracellular organelle. Arguably, structural modifications of the rotor (for example by incorporating long-alkyl chains onto the BODIPY scaffold) might allow for specific targeting of the cell organelle as well. Considering that the local microviscosity of plasma membrane/cell organelle is altered in response to external stimuli (oxidants, pore forming agents and signaling events), these molecular viscometers could be suitable for diagnostic applications. These studies are underway in our laboratories.

Acknowledgements

This work was supported by the NIH grant RO1EB12003 (ZG), NSF grant CBET-1264608 (IG), NIH grant R15AG038977 (SVD) and INFOR grant from Texas Christian University.

Notes and References

*Corresponding author: z.gryczynski@tcu.edu

[1] Department of Physics and Astronomy, Texas Christian University, Fort Worth, TX, USA, 76129

[2] Department of Cell Biology and Immunology, UNT Health Science Center, Fort Worth, TX, USA, 76107

[3] Department of Integrative Physiology and Anatomy, UNT Health Science Center, Fort Worth, TX, USA, 76107

[4] Department of Chemistry, Texas Christian University, Fort Worth, TX, USA, 76129

References

1 V. T. Turitto, *Prog. Hemost. Thromb.,* 1982, **6**, 139–177.

2 Y. N. Andrade, J. Fernandes, E. Vazquez, J. M. Fernandez-Fernandez, M. Arniges, T. M. Sanchez, M. Villalon and M. A. Valverde, *J. Cell Biol.,* 2005, **168**, 869–874.

3 M. K. Kuimova, *Phys. Chem. Chem. Phys.,* 2012, **14**, 12671–12686.

4 M. A. Haidekker and E. A. Theodorakis, *Org. Biomol. Chem.,* 2007, **5**, 1669–1678.

5 M. A. Haidekker and E. A. Theodorakis, *J. Biol. Eng.,* 2010, **4**, 11.; http://www.jbioleng.org/content/4/1/11

6 J. Fan, M. Hu, P. Zhan and X. Peng, *Chem. Soc. Rev.,* 2013, **42**, 29–43.

7 M. Kumar, N. Kumar, V. Bhalla, H. Singh, P. R. Sharma and T. Kaur, *Org. Lett.,* 2011, **13,** 1422–1425.

8 X. Cao, W. Lin, Q. Yu and J. Wang, *Org. Lett.,* 2011, **13**, 6098–6101.

9 H. Yu, Y. Xiao, H. Guo and X. Qian, *Chem. Eur. J.,* 2011, **17**, 3179–3191.

10 G. Ulrich, R. Ziessel and A. Harriman, *Angew. Chem. Int. Ed.,* 2008, **47**, 1184–1201.

11 R. Ziessel, G. Ulrich and A. Harriman, *New J. Chem.,* 2007, **31,** 496–501.

12 N. Boens, V. Leen and W. Dehaen, *Chem. Soc. Rev.,* 2012, **41**, 1130–1172.

13 A. Loudet and K. Burgess, *Chem. Rev.,* 2007, **107,** 4891–4932.

14 A. Kamkaew, S. H. Lim, H. B. Lee, L. V. Kiew, L. Y. Chung and K. Burgess, *Chem. Soc. Rev.,* 2013, **42**, 77–88.

15 A. C. Benniston and G. Copley, *Phys. Chem. Chem. Phys.,* 2009, **11**, 4124–4131.

16 J. A. Levitt, P. Chung, M. K. Kuimova, G. Yahioglu, Y. Wang, J. Qu and K. Suhling, *ChemPhysChem,* 2011, **12,** 662–672.

17 I. López-Duarte, T. T. Vu, M. A. Izquierdo, J. A. Bull and M. K. Kuimova, *Chem. Commun.,* 2014, **50**, 5282–5284.

18 J. A. Levitt, M. K. Kuimova, G. Yahioglu, P. Chung, K. Suhling and D. Phillips, *J. Phys. Chem. C,* 2009, **113**, 11634–11642.

19 Y. Wu, M. Štefl, A. Olzyńska, M. Hof, G. Yahioglu, P. Yip, D. R. Casey, O. Ces, J. Humpolíčková and M. K. Kuimova, *Phys. Chem. Chem. Phys.,* 2013, **15**, 14986–14993.

20 H. Zhu, J. Fan, M. Li, J. Cao, J. Wang and X. Peng, *Chem. Eur. J.,* 2014, **20**, 4691–4696.

21 Z. Yang, Y. He, J. Lee, N. Park, M. Suh, W. Chae, J. Cao, X. Peng, H. Jung and C. Kang, *J. Am. Chem. Soc.,* 2013, **135,** 9181–9185.

22 M. K. Kuimova, S. W. Botchway, A. W. Parker, M. Balaz, H. A. Collins, H. L. Anderson, K. Suhling and P. R. Ogilby, *Nat. Chem.,* 2009, **1**, 69–73.

23 J. D. Kimball, S. Raut, L. P. Jameson, N. W. Smith, Z. Gryczynski, S. V. Dzyuba, 2014, *submitted.*

24 A. F.López, O. P.Ruiz and A. I.López, *Chem. Phys. Lett.* 1988, **148**, 253–258.

25. L. P. Jameson, J. D. Kimball, Z. Gryczynski, M. Balaz, S. V. Dzyuba, *RSC Adv.,* 2013, **3**, 18300–18304.

26 T. Forster and G. Hoffmann, *Z. Phys. Chem,* 1971, 63-76.

27 M. Kaschke, J. Kleinschmidt and B. Wilhelmi, *Laser Chem.,* 1985, **5**, 119-132

28 K. Suhling, P. M. French and D. Phillips, *Photochem. Photobiol. Sci.,* 2005, **4,** 13–22.

29 P. Ghanouni, Z. Gryczynski, J. Steenhuis, T. Lee, D. Farrens, J. Lakowicz and B. Kobilka, *J. Biol. Chem*., 2001, **276**, 24433–24436.

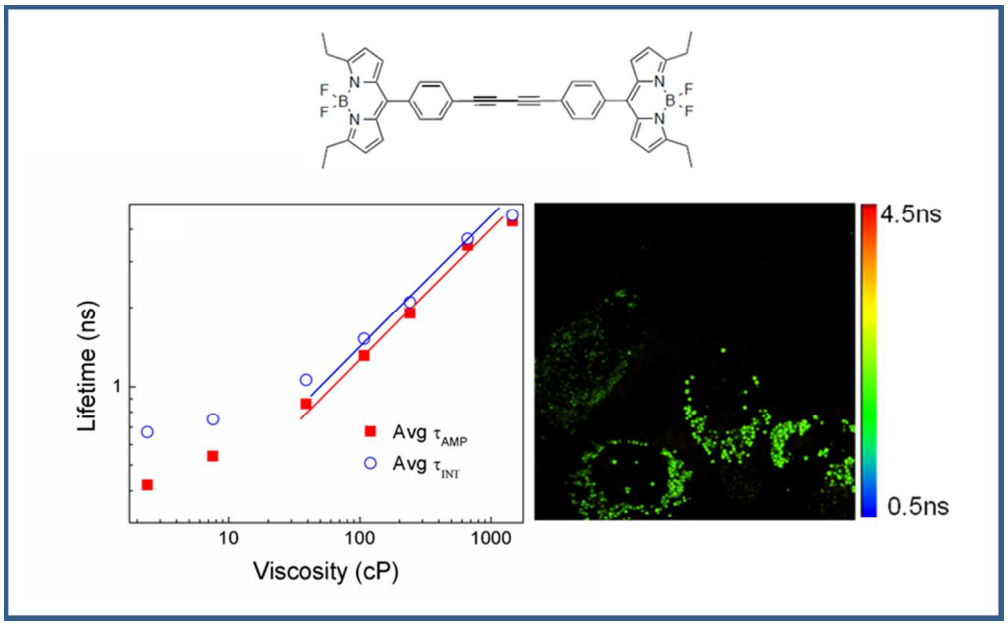

142x87mm (150 x 150 DPI)